Charge Transport and Rectification in Arrays of SAM-Based Tunneling Junctions

Citation

Published Version

Permanent link

Terms of Use

Share Your Story

Charge Transport and Rectification in Arrays of SAM-Based Tunneling Junctions

Christian A. Nijhuis, William F. Reus, Jabulani R. Barber, Michael D. Dickey, and George M. Whitesides[*]

Department of Chemistry and Chemical Biology, Harvard University, 12 Oxford St, Cambridge, MA 02138, USA

Corresponding author:

Tel.: 617 458 9430

Fax: 617 458 9857

e-mail: gwhitesides@gmwgroup.harvard.edu

Abstract. This paper describes a fabrication method that generates small arrays of tunneling junctions based on self-assembled monolayers (SAMs) with liquid metal top-electrodes and ultra-flat bottom-electrodes; the yield of junctions in this method is high (70-90%). These junctions incorporate SAMs of alkanethiolates with ferrocene termini (11-(ferrocenyl)-1-undecanethiol, $SC_{11}Fc$), and rectify currents with large rectification ratios (R) of $R = 90 - 180$. These values are larger than predicted by theory ($R \sim 20$), and larger than previous experimental measurements. SAMs of n-alkanethiolates without the Fc groups ($SC_{n-1}CH_3$, with n = 12, 14, 16, or 18) do not rectify ($R = 1.0 - 5.0$). These arrays enable the measurement of the electrical characteristics of the junctions as a

function of chemical structure, voltage, and temperature, over the range of 90 – 293 K, with statistically large numbers of data (N = 300 – 800). Rectification with Fc-terminated SAMs seems to be based on a mechanism of charge transport that changes with bias: from tunneling (at one bias), to hopping combined with tunneling (at the opposite bias).

Introduction

Molecular electronics[1] originally promised that molecule(s) bridging two or more electrodes would generate electronic function, and overcome the scaling limits of conventional semiconductor technology.[2] So far, there have been no commercially successful electronic devices employing small molecules as the active element. Fabricating even simple molecular circuits that incorporate more than a handful of molecules is a challenge: most fabrication techniques have low yields,[3] produce junctions that are dominated by artifacts[4] (especially conducting filaments[5,6,7,8]), and generate too few reliable data for statistical analysis (the work of Lee et al. provides an exception[9]). Largely absent are physical-organic studies connecting molecular structure and electrical properties, and studies that include measurements as a function of temperature – measurements necessary to determine the mechanism(s) of charge transport across SAM-based junctions (the work of Allara et al.[10] and Tao et al.[11] provide examples of successful studies). Here we describe a technique that generates small arrays (seven junctions) of SAM-based junctions with satisfactory yields (70 – 90%) of working devices; this technique makes it possible to conduct physical-organic studies with statistically large numbers of data (N = 400 – 800), and to do so over a range of temperatures (*T*) from 90 to 293 K.

We describe two systems. i) Junctions based on SAMs of n-alkanethiolates ($SC_{n-1}CH_3$); these junctions show, as expected,[4] tunneling as the dominant mechanism of charge transport. ii) Junctions based on SAMs of alkanethiolates terminated with ferrocene (11-(ferrocenyl)-1-undecanethiol, $SC_{11}Fc$) groups; these junctions rectify currents, and thus act as molecular diodes with rectification ratios $R \approx 1.3 \times 10^2$ (eq. **1**). In equation **1**, J = current density (A/cm^2) and V = voltage (V).

$$R \equiv |J(\text{-1.0 V})/J(\text{+1.0 V})| \tag{1}$$

Studying the rectification ratios, rather than current densities, has the advantage that the current measured in one direction of bias serves as a reference for the current measured at the opposite bias and, thus, eliminates many of the uncertainties related to contact resistances or contact areas. The junction at one bias is the reference for the junction at the opposite bias.

Most research, both theoretically and experimentally, that has had the objective of developing the molecular analogue of a diode has been based on the so-called "electron donor-bridge-acceptor" compounds described in a seminal paper by Aviram and Ratner.[12] Tunneling junctions incorporating these molecules,[13,14,15] and others,[16,17] (including one example reported by us[18]) have rectified currents, but neither the mechanism of charge transport nor the origin of the observed rectification have been unambiguously established in any junction. Four factors underlie this ambiguity: i) structural information on SAMs only exists for a relatively small number of molecular precursors;[19] virtually no structural information is available for SAMs incorporating molecules with the donor-bridge-acceptor architecture, due to their structural complexity. ii) Asymmetries other than an electric dipole, present in either the SAMs themselves or in the junctions, can

contribute to rectification;[20] many of the previous studies do not rule out these other possible sources of rectification using appropriate controls and statistics. iii) The reported rectification ratios have typically been low ($1 < R < 5$.[16, 17,18]). Without adequate statistical support, most of these values are not distinguishable from $R \sim 1$. iv) J(V) measurements as a function of temperature have not been conducted.[10,11,21]

These studies, as a group, have not considered molecular rectifiers in which a change occurs in the mechanism of charge transport (e.g., from tunneling to hopping) as applied bias switches from one direction to the other; we believe that such junctions have the potential to yield large rectification ratios ($R > 10^2$).

Fabrication of the Devices

We have reported that a eutectic alloy of gallium and indium (EGaIn) with its superficial layer of Ga_2O_3, can be molded into cone-shaped tips that are useful to form electrical contacts with SAMs[22,23]: the properties of Ga_2O_3/EGaIn resemble that of a non-Newtonian fluid.[24] This method affords SAM-based junctions, with high yields of working devices, and enables statistical analysis through the collection of large numbers of data. These junctions – with the top-electrode suspended from a syringe – are convenient to use, but they lack the encapsulation and addressability needed to operate in a pressure- and temperature-controlled chamber.
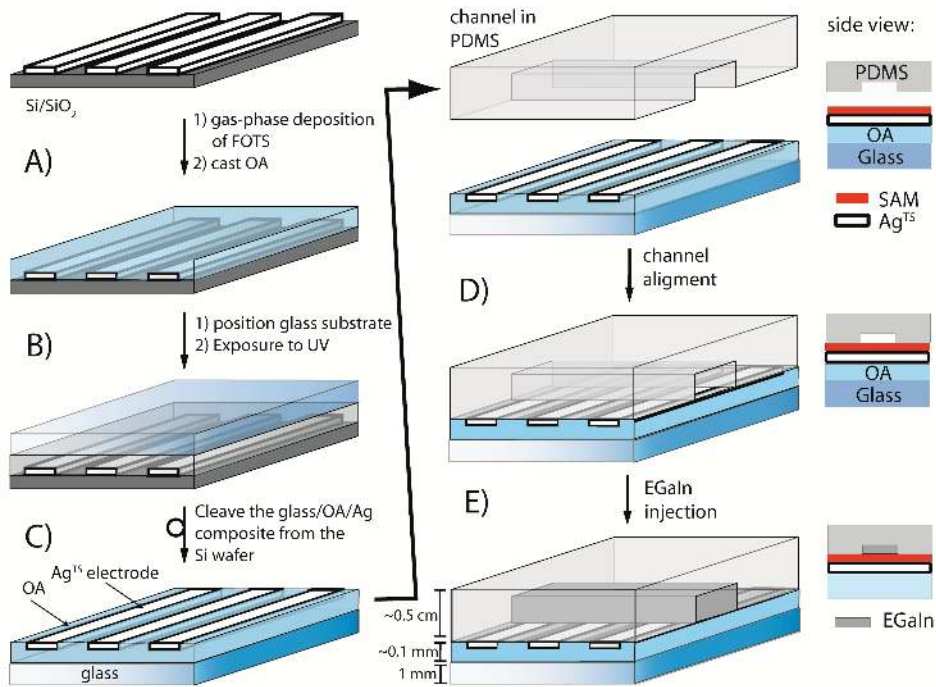
Figure 1 outlines the method, based on Ga_2O_3/EGaIn, that we used to construct arrays of SAM-based tunneling junctions that i) are mechanically stable, ii) do not suffer from alloying between metal electrodes, iii) do not require metal deposition either by electron-beam evaporation or by sputtering directly onto SAMs, iv) do not require intermediate

4

layers of conducting polymers, or rigorous/empirical processing steps, and v) make it possible to perform J(V) measurements as a function of temperature over a broad range of temperatures (90 – 293 K). This method uses Ga_2O_3/EGaIn, stabilized in microchannels in a transparent polymer (PDMS), as a liquid metal top-electrode (see Methods). Figure 2 shows optical micrographs of a complete device.
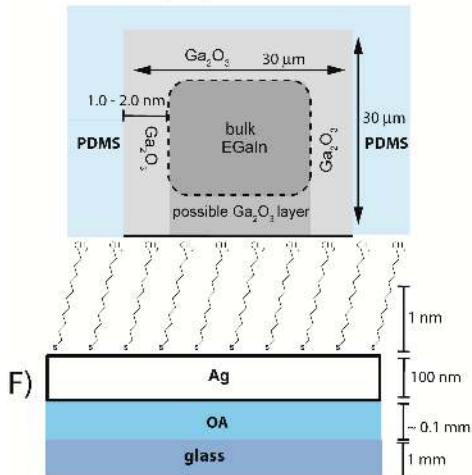
Figs. 1F and 1G show idealized views of the junctions. In reality, the SAMs have defects due to i) step edges, ii) phase boundaries, iii) pin holes, iv) impurities, and v) grain boundaries.[19] To reduce the number of defects in the SAM relative to the number present in the rough top-surface of evaporated silver, we used ultra-flat, template-striped silver (Ag^{TS}) electrodes embedded in cured optical adhesive (OA).[25] It is important to embed the electrodes in OA to prevent free-standing structures of Ag on the wafer, with edges at which the SAMs can not pack densely,[26] that may cause shorts once the channels are filled with Ga_2O_3/EGaIn.

The atomic force micrograph shows two important characteristics of these electrodes (Fig. 2). i) The difference in height between the OA and Ag electrodes was insignificant (< 0.1 nm). ii) The Ag^{TS} electrodes were smooth and had a root-mean-square surface roughness of 0.9 nm (approximately two lattice planes of silver) measured over 25×25 μm^2, but the Ag^{TS}/OA interface did not seal completely with the OA at their edges: the gap at the Ag^{TS}/OA-interface was 150 nm wide and 6.0 nm deep, with a surface roughness of 5.8 nm (averaged over $5.0 \times 0.1 \ \mu m^2$).
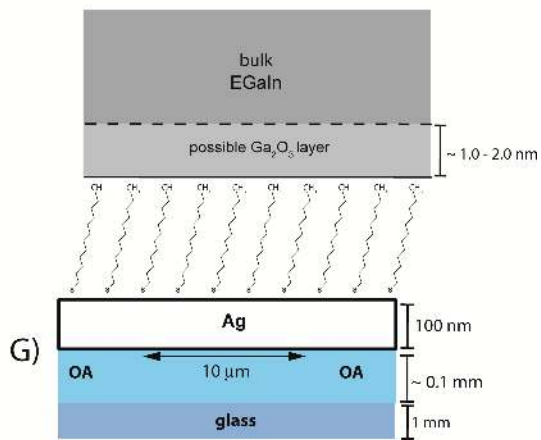
Figure 1: Fabrication of the arrays of SAM-based tunneling junctions. The schematic representations are not drawn to scale. A) We fabricated the pattern of Ag-electrodes using photolithography, electron-beam deposition of silver, and lift-off. B) Using a UV-curable adhesive, we affixed a glass substrate to the pattern of the silver electrodes. The cured optical adhesive interacts strongly with the Ag and the glass support, but not with the wafer. C) We cleaved the Ag/adhesive/glass composite from the wafer by applying a razor blade – with gentle pressure in a direction parallel to the wafer – between the glass substrate and the wafer. D) We aligned a microchannel in PDMS perpendicular to the electrodes after we formed the SAMs on these electrodes. E) We filled the microchannels with Ga_2O_3/EGaIn to complete the device. F) and G) show schematic, idealized representations of the two side views of the junctions with a SAM of $SC_{11}CH_3$. H) A schematic representation of the Ag^{TS}/OA interface. The gap between the OA and the Ag^{TS} (indicated by the red arrow), probably caused by shrinkage of the polymer during polymerization, is 150 nm wide and 6 nm deep. The SAMs will be disordered at the edge of the electrode; this disordered region has the potential to be a source of defects in the junctions. We believe that the surface tension of Ga_2O_3/EGaIn (surface tension of Ga_2O_3/EGaIn is 624 mN/m[27]) prevents it from filling the gap (filled with air) between the AO and the Ag^{TS}, but we have no direct evidence to support this belief.

A)

Si/SiO$_2$

1) gas-phase deposition of FOTS
2) cast OA

B)

1) position glass substrate
2) Exposure to UV

C)

Cleave the glass/OA/Ag composite from the Si wafer

OA   Ag^{TS} electrode

glass

channel in PDMS

D)

channel aligment

E)

EGaIn injection

~0.5 cm

~0.1 mm

1 mm

side view:

PDMS

OA
Glass

SAM
Ag^{TS}

OA
Glass

EGaIn

Cross section perpendicular to channel:

Ga$_2$O$_3$ 30 μm

1.0 - 2.0 nm

PDMS   Ga$_2$O$_3$ bulk EGaIn   Ga$_2$O$_3$ PDMS

30 μm

possible Ga$_2$O$_3$ layer

1 nm

Ag   100 nm

OA   ~ 0.1 mm

glass   1 mm

F)

Cross section parallel with channel:

bulk EGaIn

possible Ga$_2$O$_3$ layer   ~ 1.0 - 2.0 nm

Ag   100 nm

OA   10 μm   OA   ~ 0.1 mm

glass   1 mm

G)

The Ag^{TS}/OA interface:

bulk EGaIn   Defects

~1.0 - 2.0 nm   possible   Ga$_2$O$_3$ layer   bulk EGaIn

1.5 nm   possible Ga$_2$O$_3$ layer

150 nm

Air or
Ga$_2$O$_3$/EGaIn

~0.5 nm
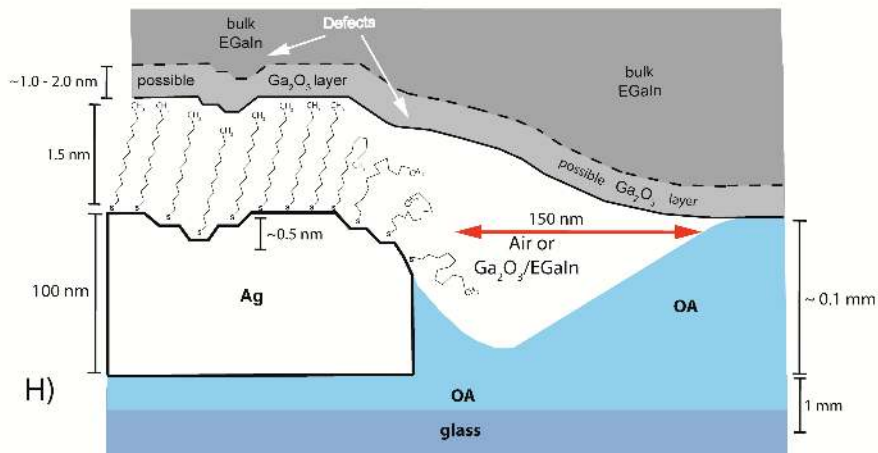
100 nm   Ag   OA   ~ 0.1 mm
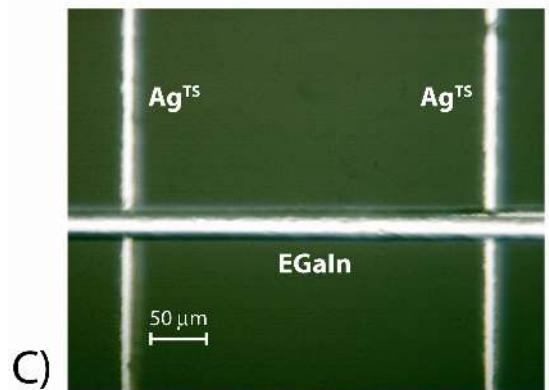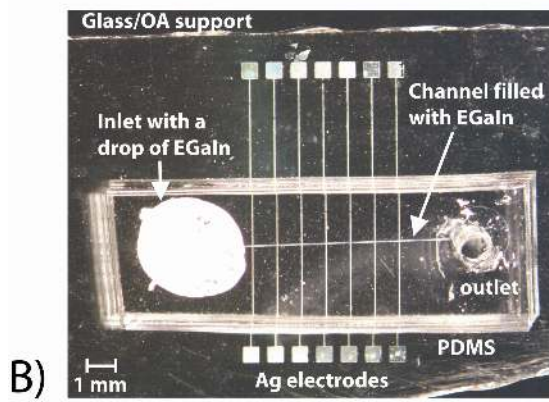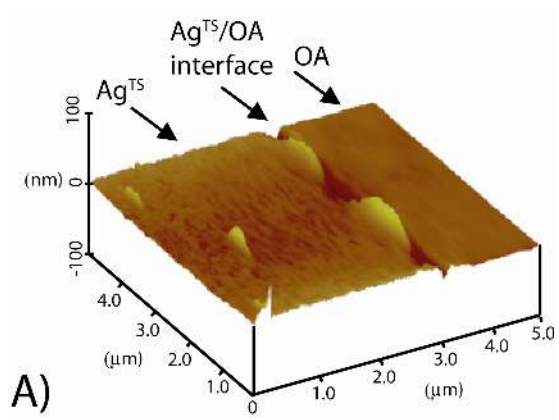
OA   1 mm

glass

H)

7

Figure 2: Atomic force microscopy images of the Ag^{TS} electrodes and optical micrographs of a complete device. A) Atomic force micrograph of the Ag^{TS}/AO interface. B) Optical micrograph of a complete device. C) Magnification of two junctions.

A)

B)

C)

This procedure, thus, generates embedded electrodes that are flat, but the topography at the interface between the metal and OA is not completely smooth. Figure 1H sketches this AO/Ag^{TS} interface schematically.

Statistical Analysis.

To account for defects in the tunneling junctions, to discriminate artifacts from real data, and to determine the yields of working devices, we believe it is essential to collect, and to analyze statistically, large numbers of data.[9] Although statistical analyses are common in (and an essential part of) studies involving break junctions,[30] and junctions involving scanning probes,[11] Lee et al.[9] was the first to address, with statistical analysis of many data, the shortcomings of SAM-based junctions having evaporated metal top-electrodes prepared using the very low-yielding procedures reported in most prior work.

We used a procedure for the statistical analysis of the data that we have described previously (see Additional Information and Methods).[23] We constructed histograms of *all* values of *J* for each measured potential. We fitted *all* our data to single Gaussian functions using a non-linear least squares fitting procedure to obtain the log-mean value of *J* for each measured potential, and its log-standard deviation. We emphasize that no data are omitted: we have *not* selected data.

Junctions with SAMs of SC$_{n-1}$CH$_3$

Figures 3A and B show, as expected from a large body of previous work, that the current density through SAMs of alkanethiols[4,9,31,32,33] i) depends exponentially on the thickness (*d* (Å)) of the SAM, ii) depends linearly on the bias in the low-bias regime, and

iii) is independent of the temperature T. All these observations indicate that the mechanism of charge transport is tunneling. The tunneling decay coefficient β (Å^{-1}) can be determined using eq. **2** (J_0 (A/cm^2) is a constant that depends on the system and includes contact resistance).

$$J = J_0 e^{-\beta d} \tag{2}$$

We found that $\beta = 0.80 \pm 0.2 \text{ Å}^{-1}$ (or $\beta = 1.0 \pm 0.2$ per CH_2) with $J_0 = 6.3 \times 10^2 \text{ A/cm}^2$ at a bias of -0.5 V and $\beta = 0.74 \pm 0.2 \text{ Å}^{-1}$ (or $\beta = 0.93 \pm 0.2$ per CH_2) with $J_0 = 21 \text{ A/cm}^2$ at -0.2 V; both values of β are within the range reported for similar compounds,[4] including those obtained with cone-shaped tips of Ga_3O_2/EGaIn.[22] (Our initial description[22] of these cone-shaped electrodes gave values of J that we interpreted to indicate a significantly lower value: $\beta = 0.6$ per CH_2. We now believe this interpretation was incorrect, and that a value of $\beta = 1.0$ per CH_2 is correct. We will discuss the origin of this error in a separate paper.[34]). Figure 3A shows a temperature-dependent measurement of J(V) of a Ag^{TS}-$SC_{13}CH_3$//Ga_2O_3/EGaIn junction (see Methods; "TS" = template stripped). The devices we used in this study could be cooled from 293 K to 110 K, and warmed again to 293 K, without changing their J(V) characteristics (in vacuum at 1×10^{-6} bar). From this experiment we conclude that neither i) solidification of EGaIn at ~ 250 K, nor ii) the differences between the thermal expansion coefficients for PDMS (3×10^{-4}/K),[35] glass (0.08×10^{-4}/K),[36] Ga_2O_3 ($0.042 \times 10^{-4} \text{ K}^{-1}$),[37] Ag ($0.18 \times 10^{-4}$/K),[38] and EGaIn ($1.1 \times 10^{-4}$/K)[39] cause shorts, lead to loss of contact, or alter the device characteristics in destructive ways.

Figure 3: Current density measurements of Ag^{TS}-$SC_{13}CH_3$//Ga_2O_3/EGaIn and Ag^{TS}-$SC_{11}Fc$//Ga_2O_3/EGaIn junctions. A) Four J(V) curves of a Ag^{TS}-$SC_{13}CH_3$//Ga_2O_3/EGaIn junction measured at four different temperatures ($T = 110, 190, 250$, and 293 K) in vacuum (1×10^{-6} bar). Inset, the current density vs. the voltage in the low-bias regime (-0.10 to 0.10 V). B) The values of J measured at -0.5 and -0.2 V as a function of the length of the SAM. The black, solid lines are fits to eq. **2**. C) A semi-log plot of the average absolute value of the current density vs. the voltage of Ag^{TS}-$SC_{11}Fc$//Ga_2O_3/EGaIn junctions. The error bars indicate the log-standard deviation. At low voltages we observed a non-zero current (see Additional information). The current could involve oxidation-reduction processes of the Fc moieties. We did not observe (or perhaps too small to be observed) those currents in junctions with SAMs of $SC_{n-1}CH_3$. Inset, the histogram of the rectification ratios with a Gaussian fit to this histogram. We did not select data prior to analysis, and the Gaussian function is a fit to all data (see additional information for details). D) Three J(V) curves measured at three different temperatures ($T = 110, 250$, and 293 K).
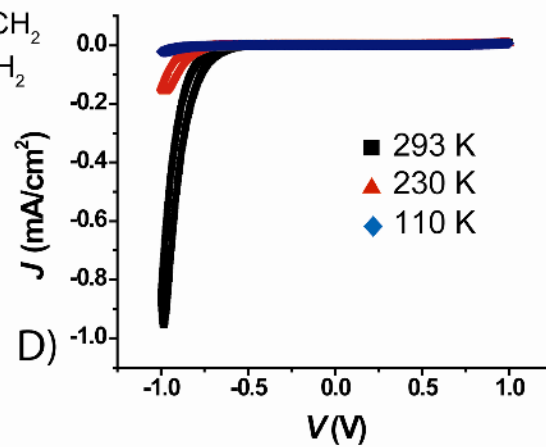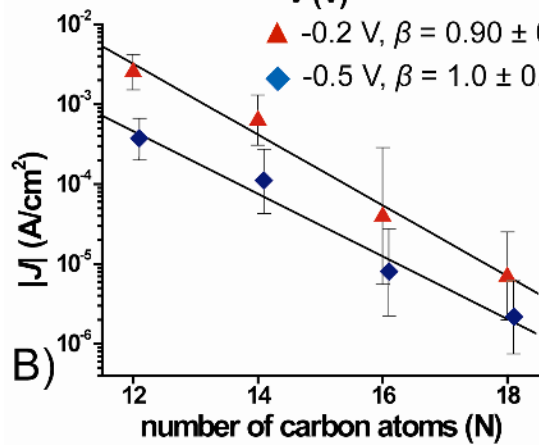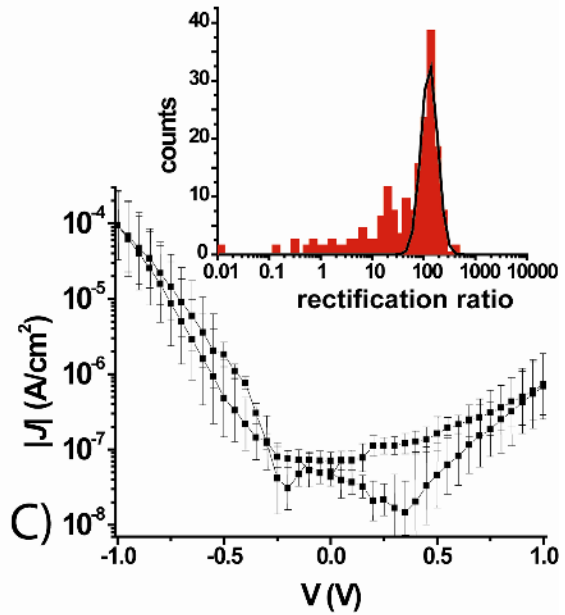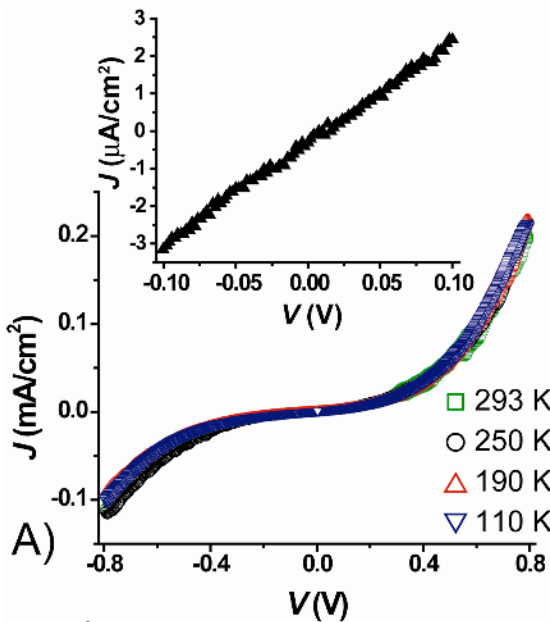
The Layer of Ga$_2$O$_3$

The junctions have three uncertainties all related to the layer of Ga$_2$O$_3$. i) *The resistance of the layer of Ga$_2$O$_3$*: we estimated the resistance of the layer of Ga$_2$O$_3$ and concluded that the resistance is approximately four orders of magnitude less than that of a SAM of SC$_{10}$CH$_3$ (see Additional Information).[23] ii) *The thickness of the layer of Ga$_2$O$_3$*: we measured the thickness of the layer of Ga$_2$O$_3$ on a drop of Ga$_2$O$_3$/EGaIn to be less than 2.0 nm (see Additional Information).[24] iii) *The topography of contact of Ga$_2$O$_3$/EGaIn with the SAM*: we recorded optical micrographs of the Ga$_2$O$_3$/EGaIn in microchannels in PDMS sealed against glass surfaces which suggest that the Ga$_2$O$_3$/EGaIn forms a conformal contact with the glass surface.

We believe that a layer of Ga$_2$O$_3$ at the PDMS interface forms during filling of the channels, since PDMS is permeable to oxygen.[24] This layer interacts strongly with the walls of the microchannel and is important for stabilizing the EGaIn in the microchannel (EGaIn has a higher surface tension than Hg, but Hg – because its surface tension is not lowered by formation of an oxide layer -- does not form stable features in microchannels in PDMS).[24] We have no direct evidence describing the interface between the Ga$_2$O$_3$/EGaIn and the SAM, but we infer that a discontinuous layer of Ga$_2$O$_3$ forms at this interface (see Additional Information). In our discussions we assume that the layer of Ga$_2$O$_3$ is present. In any case, a layer of Ga$_2$O$_3$ may influence the values of J, but it will not influence the value of R, because the value of R is the ratio of the current densities measured at opposite bias across the same junction (eq. **1**).

Junctions with SAMs of SC$_{11}$Fc

Figure 3C shows the average current density as a function of voltage for the Ag^{TS}-$SC_{11}Fc//Ga_2O_3/EGaIn$ junctions, and the histogram of the rectification ratios with a Gaussian fit to this histogram. These junctions show large rectification ratios (eq. **1**, $R \approx$ 1.3×10^2 with a log-standard deviation of 1.4). Thus, 68% of the log-normal distribution of R lies within the interval (90,180).

The junctions have three sources of asymmetry that may contribute to the rectification. i) The two contacts between the electrodes and the SAMs differ: the $Ga_2O_3/EGaIn$ top-electrode forms a van der Waals contact, and the silver bottom-electrode forms a covalent $Ag-S-CH_2$ contact. ii) The top- ($Ga_2O_3/EGaIn$) and bottom-(Ag) electrodes may have different work functions ($\Phi_{Ag} \approx \Phi_{EGaIn} \approx 4.5$ eV, but the work functions of each surface may be modified by the SAM or Ga_2O_3, respectively). iii) A layer of Ga_2O_3 is present only on the top-electrode, and not on the bottom-electrode. We believe that the rectification in the Ag^{TS}-$SC_{11}Fc//Ga_2O_3/EGaIn$ junctions is due to the molecules, and not to any other asymmetries in our junctions or redox reactions involving Fc and GaO_x,[23] for two reasons: i) junctions lacking the Fc moiety – e.g., with SAMs of $SC_{n-1}CH_3$ – do not rectify; thus, neither the layer of Ga_2O_3 itself nor any other asymmetries in the junctions cause rectification. ii) Two types of junctions with SAMs of $SC_{11}Fc$ having top-electrodes other than $Ga_2O_3/EGaIn$ – namely, a tungsten STM tip[46] and a redox-inactive Au foil[23] – also rectified currents with values of $R \sim 10 - 100$.

Temperature-Dependent Measurements of Ag^{TS}-$SC_{11}Fc//Ga_2O_3/EGaIn$ Junctions

To clarify the mechanisms of charge transport across the Ag^{TS}-$SC_{11}Fc//Ga_2O_3/EGaIn$ junctions, we measured the dependence of $J(V)$ on temperature. Figure 3D shows three

15

J(V) curves measured at 110, 230, and 293 K and Fig. 4A shows both the values of *J* at +1.0 V and -1.0 V for the Ag^{TS}-$SC_{11}Fc$//Ga_2O_3/EGaIn junctions measured at $T = 110$ to 293 K. The values of *J* depend on *T* at negative bias, but are independent of *T* at positive bias. This observation indicates that tunneling (which is temperature independent) is the dominant mechanism of charge transport at positive bias, while hopping (which follows an Arrhenius dependence on temperature, see below) is the dominant mechanism of charge transport at negative bias. This observation also illustrates the value of examination of rectification: whatever the uncertainties about a junction, its behavior at one bias is an excellent control for its behavior at opposite bias. Here, the comparison of forward and reverse bias at different temperatures supports the conclusion that cooling the devices does not introduce artifacts into our measurements.

Figure 4 shows the Arrhenius plots of the Ag^{TS}-$SC_{11}Fc$//Ga_2O_3/EGaIn junction at potentials in the range of -0.40 to -1.0 V and 0.40 to 1.0 V. This plot yields three important pieces of information. i) Hopping is only observed between -0.60 and -1.0 V, while at all other measured potentials the dominant mechanism of charge transport is tunneling; this observation suggests that at -0.60 V the HOMO of the Fc begins to contribute to charge transport. ii) The activation energy, determined from the slope of the Arrhenius plot using eq. **3** (where the Boltzmann constant $k_B = 8.62 \times 10^{-5}$ eV K^{-1}) is $E_a = 77 \pm 5.3$ meV (7.4 ± 0.51 kJ/mol) and is independent of the temperature. iii) At temperatures below 190 K, $k_B T \leq 16$ meV and is much smaller than E_a (77 ± 5.3 meV). Hence, at $T < 190$ K, tunneling is the dominant mechanism of charge transport over the entire range of applied bias (-1.0 V to 1.0 V).

$$j = j_0 \exp(- E_a / k_B T) \tag{3}$$

The Mechanism of Rectification

All these observations can be rationalized by the model of charge transport proposed in Figure 5. This Figure shows proposed energy-level diagrams of the Ag^{TS}-$SC_{11}Fc//Ga_2O_3/EGaIn$ junctions at biases of -1.0 and 1.0 V. In all experiments, we biased the $Ga_2O_3/EGaIn$ top-electrodes, and grounded the Ag^{TS} bottom-electrode. The HOMO level of the $SC_{11}Fc$ is centered on the Fc moiety, and couples more strongly to the $Ga_2O_3/EGaIn$ top-electrode than to the Ag^{TS} bottom-electrode, because it is in van der Waals contact with the $Ga_2O_3/EGaIn$ electrode, but it is separated from the Ag^{TS} electrode by the SC_{11} group. At positive bias, the Fermi level of the $Ga_2O_3/EGaIn$ top-electrode decreases to below the value of the Fermi level of the Ag^{TS} electrode. The HOMO of the Fc follows the Fermi level of the top-electrode, and therefore does not fall between the Fermi levels of the two electrodes. It does not participate in charge transport, but instead it becomes part of the tunneling barrier.

At negative bias, the Fermi level of the top-electrode increases, as does the HOMO of the Fc. At sufficiently negative bias, the HOMO of the Fc can overlap with both Fermi levels of the electrodes, and contribute to charge transport. We do not know all the details of the mechanism of charge transport, but we speculate that, when the HOMO level of the Fc is accessible, the first step involves an electron from the HOMO level of the Fc tunneling across the SC_{11} moiety (resulting in an Fc^+-ion), and the second step involves an electron hopping across the Fc moiety, as suggested by the arrows (the arrows would point in the opposite direction in the case of hole transport).

Figure 4: Thermally activated charge transport across Ag^{TS}-$SC_{11}Fc$//Ga_2O_3/EGaIn junctions. A) The values of J measured at -1.0 and 1.0 V as a function of temperature. Arrhenius plot of Ag^{TS}-$SC_{11}Fc$//Ga_2O_3/EGaIn junction for values of J measured at different potentials as a function of temperature in the range of -0.40 V to -1.0 V (B) and 0.40 to 1.0 V (C). The red dashed vertical line indicates the temperature at which the EGaIn solidifies (as we could observe when we contacted the Ga_2O_2/EGaIn electrode with the probe). The solid black lines are fits to eq. **3** and indicate regimes where the mechanism of charge transport is dominated by hopping. The dashed black lines are guides to the eyes to indicate regimes where the mechanism of charge transport is dominated by tunneling.
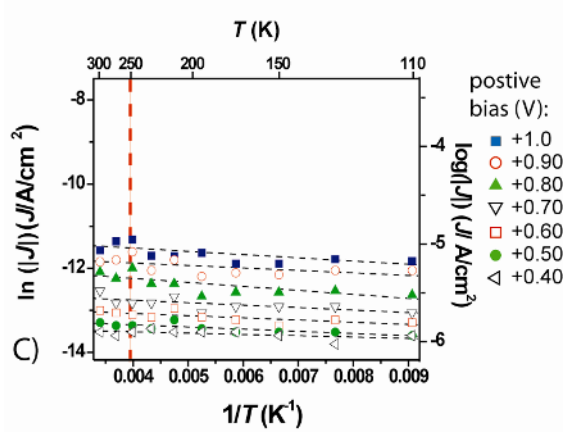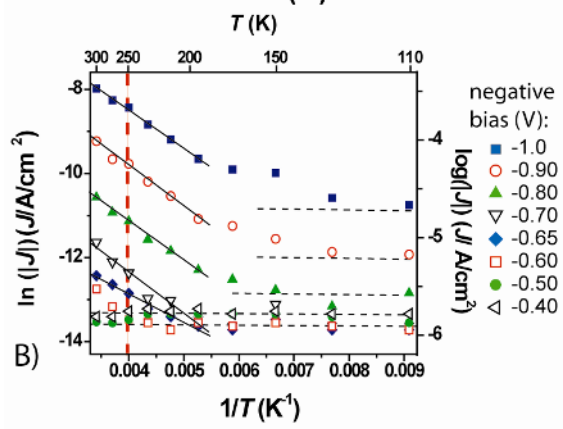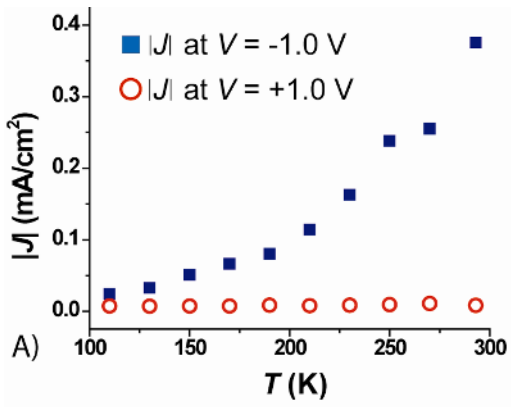
Activation of the hopping mechanism at negative bias led to values of J that were two orders of magnitude higher (at room temperature) than those observed with tunneling alone at positive bias; thus, in our junctions, hopping is more efficient in the transport of charge than tunneling (Fig. 4). We infer that tunneling is the rate-limiting step in the transport of charge, and that the life-time of the Fc^+ species is probably short. We do not know how many Fc groups are oxidized at any given time, or how the Fc^+-ions interact with Ga_2O_3-layer. The Fc^+-ions will probably have a stronger interaction (perhaps ionic) with the Ga_2O_3-layer than neutral Fc moieties. We believe that the layer of Ga_2O_3 does not significantly affect the mechanism of charge transport across the SAMs (see above and Additional Information).

The Large Value of R

The large observed rectification ratio ($R \approx 130$) for the Ag^{TS}-$SC_{11}Fc$//Ga_2O_3 /EGaIn junctions cannot be explained solely either by the presence of an asymmetrical tunneling barrier within the junction, or by citing the difference in potential drops across the Fc moiety and the alkyl chain. Theoretical studies incorporating either of these effects have suggested that for molecular tunneling junctions, the rectification ratios can not exceed ~ 20.[47] Those studies did not, however, consider a change in the mechanism of charge transport between forward and reverse bias as a mechanism that might result in high rectification ratios.

Figure 5: Energy level diagram and mechanism of charge transport across Ag^{TS}-$SC_{11}Fc//Ga_2O_3/EGaIn$ junctions. The barrier widths of the junctions are defined by the lengths of the C_{11} alkyl chains and the Fc moiety. At positive bias, the arrows suggest that the charge traversing the junctions has to tunnel across the whole length of the molecule (C_{11} alkyl chain and Fc group; a distance of 2 nm), because the HOMO level of the Fc moiety does not overlap with the Fermi levels of the electrodes. At negative bias, the HOMO level of the Fc moiety can participate in charge transport, and the charge only has to tunnel across the C_{11} moiety over a distance of 1.3 nm. In a second step, the charge can hop across the Fc moiety. We estimated the value of the HOMO level of the Fc moiety with wet electrochemistry (see Additional Information).
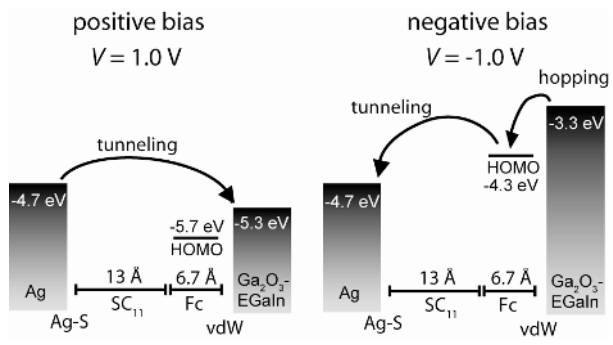
The values of R can be rationalized by the fact that hopping (when $k_B T \geq E_a$) is more efficient in the transport of charge (i.e. allows for a higher current) than tunneling (Figure 4). When the HOMO of the Fc does not participate in charge transport, the charge must tunnel (elastically or inelastically) through the entire width of the junction, i.e., roughly the whole length of $SC_{11}Fc$ molecule defined by the lengths of the SC_{11} chain (d_{SC11}, 1.3 nm) and the Fc moiety (d_{Fc}, 0.66 nm). When the HOMO of the Fc falls between the Fermi levels of the electrodes, charge can tunnel from the HOMO of the Fc across the C_{11} chain, followed by hopping across the Fc moiety. This change in the mechanism of charge transport from tunneling to hopping effectively reduces the width of the tunneling barrier from $d_{SC11} + d_{Fc}$ to d_{SC11}. Thus, the rectification ratio is approximately the ratio of the tunneling current densities across the whole SAM (J_{SC11Fc}) to the tunneling current density across the SC_{11} moiety (J_{SC11}) and can be estimated using eq. **6** (with β_{SC11} = the decay constant across SC_{11} (Å^{-1}, or per CH_2) and β_{Fc} = the decay constant across the Fc moiety (Å^{-1}, or per CH_2)):

$$R = J_{SC_{11}} / J_{SC_{11}Fc} \propto \exp(-\beta_{SC_{11}} d_{SC_{11}}) / \left(\exp(-\beta_{SC_{11}} d_{SC_{11}}) \exp(-\beta_{Fc} d_{Fc}) \right) \qquad \textbf{(6)}$$

We do not know the value of β_{Fc}, but have assumed $\beta_{alkyl} = \beta_{Fc} = 0.80 \text{ Å}^{-1}$ (or 1.0 per CH_2) to obtain a lower-limit value of $J_{SC_{11}} / J_{SC_{11}Fc} = 2.0 \times 10^2$. This semi-quantitative theoretical estimation of R is compatible with the observed rectification ratio of $R \approx 1.3 \times 10^2$. This proposed model also agrees with the observation that the rectification ratios are close to unity at temperatures less than 190 K (Fig. 4A), because hopping becomes less efficient than tunneling when $k_B T \ll E_a$. At low temperatures, therefore, the hopping mechanism is eliminated and the Fc moiety becomes part of the tunneling barrier in both directions of bias.

Conclusions

To realize potential applications of SAM-based devices, the mechanisms of charge transport across these SAM-based junctions must be understood. This paper describes a method of fabricating arrays of seven SAM-based junctions per device that relies on the stabilization of liquid-metal electrodes in microchannels. This method achieves high post-fabrication yields (70-90%) and junctions that are stable up to hundreds of cycles. Furthermore, this technique enables the measurement of $J(V)$ characteristics as a function of the chemical structure of the SAM, with statistically large numbers of data, and as a function of temperature over the range of $90 - 293$ K. We believe that such studies are required to confirm that the characteristics of molecular devices are indeed dominated by the chemical composition of the SAMs, to discriminate artifact from real data, and to establish the mechanism of charge transport across SAMs.

We characterized two types of SAM-based junctions incorporating SAMs of $SC_{n-1}CH_3$ (n = 12, 14, 16, and 18) and $SC_{11}Fc$. Junctions incorporating SAMs of $SC_{11}Fc$ have large rectification ratios of $R \approx 1.3 \times 10^2$, while those with SAMs of $SC_{n-1}CH_3$ do not rectify ($R \approx$ 1-5). Our physical-organic study with statistically large numbers of data (N $= 300 - 800$) show that the rectification is due to the chemical structure of the SAM, and not caused by any of the other asymmetries of the junctions. Although molecular rectifiers have been reported before,[13,14,15,16,18,20] no measurements of $J(V)$ as a function of temperature have been conducted, leaving the mechanism of charge-transport unclear. Here, measurements of $J(V)$ as a function of temperature clearly suggest a mechanism of charge transport across the Ag^{TS}-$SC_{11}Fc$//Ga_2O_3/EGaIn junctions (Figure 5) consisting of

tunneling supplemented by hopping at temperatures above 190 K and biases from -0.6 V

to -1.0 V. The charge can hop across the Fc moiety when the HOMO of the Fc overlaps

with the Fermi levels of the electrodes, and thus reduces the width of the tunneling

barrier, an event which occurs at negative bias but not positive bias. Thus, a difference in

the mechanism of charge transport at opposite biases across the *same* junction is the basis

of the large molecular rectification ($R \approx 1.3 \times 10^2$) we observe in this system, and is

potentially useful for constructing other molecular- or SAM-based, two-terminal devices

with well-defined electronic functions.

Methods

Preparation of the SAMs. The synthesis of $HSC_{11}Fc$ followed a procedure described in

the literature.[49] The $HSC_{n-1}CH_3$ (with n = 12, 14, 16, or 18, Sigma Aldrich) was purified

by recrystallization from ethanol (under N_2, three times) prior to its use in the formation

of the SAMs. We formed the SAMs at the Ag^{TS} surfaces on glass (or on Au^{TS} surface on

glass for electrochemical studies) using 1-2 mM ethanolic solutions of the corresponding

thiols under nitrogen over 16 h.

Device Fabrication. We used photolithography, e-beam evaporation, and standard lift-

off processes to form arrays of 100 nm thick Ag electrodes (10 μm wide and 5000 μm

long, with $500 \times 500 \ \mu m^2$ square pads at their ends that facilitated addressing the

electrodes with probes) on Si/SiO_2 wafers.

The optical adhesive (OA, Norland, No. 61) adheres strongly to Si/SiO_2. To

minimize this interaction and to allow successful template stripping (TS), we

functionalized the wafer with a monolayer of 1H,1H,2H,2H-perfluorooctyl-

trichlorosilane ($Cl_3Si(CH_2)_2(CF_2)_5CF_3$, FOTS) by gas phase deposition of the FOTS for

one hour.

We applied a drop of OA as a liquid (as a film ~0.1 mm thick) on the Ag electrodes,

and positioned freshly cleaned glass slides (VWR microslides, 1 mm thick, rinsed with

EtOH followed by 5 min cleaning in a plasma of air at 500 mTorr) on top of this drop of

OA. We cured the OA for two hours in UV, during which the OA polymerized and

adhered to both the Ag and the glass support, but not to the wafer with a monolayer of

FOTS.

We separated the glass/OA/Ag composite from the Si/SiO_2 template by applying

razor blade (almost) orientated in the plane of Si-wafer to one of the corners of the

glass/OA/Ag composite. The sharp side of the razor blade was positioned against

interface defined by the OA and the Si/SiO_2 wafer (with a monolayer of FOTS). Forcing

the razor blade in between the layer of OA and the Si/SiO_2 wafer by pressing gently (in a

direction parallel to the wafer) caused the razor blade to move in between the OA and the

Si/SiO_2 wafer, and separated the glass/OA/Ag composite from the Si/SiO_2 template.

Flipping the glass/OA/Ag composite exposed the ultra-flat silver electrodes that were

originally in contact with the Si/SiO_2 wafer (Fig. 1G).[50] We immersed the electrodes in

the ethanolic solutions of the thiols which we kept under an atmosphere of N_2 within 5 s

after template-stripping to minimize contamination of the metal surfaces.

Oxidation of the PDMS with an air-plasma (500 mTorr, 60 s) prior to alignment

improved the interaction of the Ga_2O_3 with the PDMS inside the microchannels. We

positioned the microchannels (30 μm wide, 30 μm deep, and 8000 μm long) in PDMS

perpendicularly to the electrodes. The PDMS formed a contact with the OA/Ag^{TS} surface

that was strong enough to withstand further handling, and provided enough mechanical

stability to withstand everyday handling in the lab; it also was sufficiently stable to

perform J(V) measurements as a functions of temperature. We filled the microchannel

with EGaIn by applying reduced pressure (500 Torr) to the outlet of the channel with a

drop of Ga_2O_3/EGaIn at the inlet of the channel. To facilitate contact with the outlet of

the channel in PDMS, we fitted a metal tube to one end of a rubber hose, the other end of

which was connected to house vacuum. The vacuum was just enough to force the EGaIn

through the channel. We believe that metallic EGaIn fills the channels and that,

afterwards, a layer of Ga_2O_3 forms at the surface of EGaIn (see Additional Information).

We applied and removed the vacuum gently, for we found that applying large forces on

the PDMS (with the channel filled with Ga_2O_3/EGaIn) resulted in shorts. During filling,

the Ga_2O_3/EGaIn behaves as a liquid and readily fills the channel, but returns to its elastic

state once the channel is filled and atmospheric pressure is restored.[24] We hypothesize

that the strong interaction of the Ga_2O_3 with the oxidized PDMS inside the microchannels

resulted in mechanically stable structures (see Additional information).

Temperature-Dependent Measurements of J(V). In all of our measurement we biased

the Ga_2O_3/EGaIn top-electrodes and grounded the Ag^{TS} bottom-electrode. We measured

J as a function of V at different values of temperature on junctions that had their J(V)

characteristics within one log-standard deviation from the mean value of J. The

temperature dependent measurements were performed with a probe station (Desert

Cryogenics) in vacuum (1×10^{-6} bar). The devices were cooled with liquid nitrogen from

293 to 80 K over the course of three hours. We observed that during cooling the EGaIn

solidified at temperatures of 240 – 260 K. Reducing the pressure or cooling the devices

did not result in short or open circuits. At intervals of 20 K we contacted the Ag^{TS} and

Ga$_2$O$_3$/EGaIn electrodes with the probes and recorded one J(V) curve while keeping the

temperature constant. The electrodes were not contacted with the probes during cooling

or heating of the devices.

Statistical Analysis. We analyzed SAM-based tunneling junctions fabricated with SAMs

of SC$_{n-1}$CH$_3$, using statistically large numbers of J(V) curves ($N = 400 – 800$, Table S1)

for each type of SAM. The yield of working devices was 70-90%. We plotted the values

of J measured at all potentials (-0.50 to 0.50 V in steps of 50 mV) in histograms and

found that the values of J were log-normally distributed and characterized by the log-

mean (eq. **7**, where N is the number of values of J), rather than normally distributed and

characterized by the mean (eq. **8**).

$$< J >_{\log} = 10^z \quad \text{with} \quad z = \frac{1}{N} \sum_{i=1}^{N} \log_{10} |J_i| \qquad (7)$$

$$< J > = \frac{1}{N} \sum_{i=1}^{N} J_i \qquad (8)$$

To these histograms, we fitted Gaussians to obtain the log-mean for J and log-standard

deviation (see Additional Information).

References

[1] A molecular device is truly molecular if it has at least one of the dimensions of a thickness of one molecule. Single molecule junctions are junctions that ideally contain only one molecule. Junctions based on self-assembled monolayers (SAMs) contain a large number of molecules ($10^3 - 10^{12}$ depending on the size of the junctions) in the *xy*-plane, but are only one molecule thick in the *z*-direction.

[2] Collier, C. P.; Wong, E. W.; Belohradsky, M.; Raymo, F. M.; Stoddart, J. F.; Kuekes, P. J.; Williams, R. S.; Heath, J. R. *Science* **1999**, *285*, 391.

[3] Bang, G. S.; Chang, H.; Koo, J. –R.; Lee, T.; Advincula, R. C.; Lee, H. *Small* **2008**, *4*, 1399.

[4] Akkerman, H. B.; de Boer, B. *J. Phys.: Condens. Matter* **2008**, *20*, 013001.

[5] Fisher, G. L.; Walker, A. V.; Hooper, A. E.; Tighe, T. B.; Bahnck, K. B.; Skriba, H. T.; Reinard, M. D.; Haynie, B. C.; Opila, R. L.; Winograd, N.; Allara, D. L. *J. Am. Chem. Soc.* **2002**, *124*, 5528.

[6] Walker, A. V.; Tighe, T. B.; Cabarcos, O. M.; Reinard, M. D.; Haynie, B. C.; Uppili, S.; Winograd, N.; Allara, D. L. *J. Am. Chem. Soc.* **2004**, *126*, 3954.

[7] Beebe, J. M.; Kushmerick, J. G. *Appl. Phys. Lett*. **2007**, *90*, 083117.

[8] Lau, C. N.; Stewart, D. R; Williams, R. S.; Bockrath, M. *Nano Lett.,* **2004**, 4, 569.

[9] Kim, T. –W.; Wang, G.; Lee, H.; Lee, T. *Nanotechnology* **2007**, *18*, 315204.

[10] Selzer, Y.; Cabassi, M. A.; Mayer, T. S.; Allara, D. L. *J. Am. Chem. Soc*. **2004**, *126*, 4052.

[11] Li, X. L.; Hihath, J.; Chen, F.; Masuda, T.; Zang. L.; Tao, N. J. *J. Am. Chem. Soc.* **2007**, *129*, 11535.

[12] Aviram, A.; Ratner, M. A. *Chem. Phys. Lett.* **1974**, *29*, 277.

[13] Metzger, R. M. *Acc. Chem. Res.* **1999**, *32*, 950.

[14] Lenfant, S.; Krzeminski, C.; Delerue, C.; Allan, G.; Vuillaume, D. *Nano Lett.* **2003**, *3*, 741.

[15] Ashwell, G. J.; Urasinska, B.; Tyrrell, W. D. *Phys. Chem. Chem. Phys.* **2006**, *8*, 3314.

[16] Chen, X.; Jeon, Y. –M.; Jang, J. –W.; Qin, L.; Huo, F.; Wei, W.; Mirkin, C. A. *J. Am. Chem. Soc.* **2008**, *130*, 8166.

[17] Böhme, T.; Simpson, C. D.; Müllen, K., Rabe, J. P. *Chem. Eur. J.* **2007**, *13*, 7349.

[18] Chabinyc, M. L.; Chen, X.; Holmlin, R. E.; Jacobs, H.; Skulason, H.; Frisbie, C. D.; Mujica, V.; Ratner, M. A.; Rampi, M. A.; Whitesides, G. M. *J. Am. Chem. Soc.* **2002**, *124*, 11730

[19] Love, J. C.; Estroff, L. A.; Kriebel, J. K.; Nuzzo, R. G.; Whitesides, G. M. *Chem. Rev.* **2005**, *105*, 1103.

[20] Metzger, R. M. *Chem. Rev.* **2003**, *103*, 3803.

[21] Selzer, Y.; Cabassi, M. A.; Mayer, T. S.; Allara, D. L. *Nanotechnology* **2004**, *15*, S483.

[22] Chiechi, R. C.; Weiss, E. A.; Dickey, M. D.; Whitesides, G. M. *Angew. Chem. Int. Ed.* **2008**, *47*, 142.

[23] Nijhuis, C. A; Reus, W. F.; Whitesides, G. M. *J. Am. Chem. Soc.* **2009**, 131, 17814.

[24] Dickey, M. D.; Chiechi, R. C.; Larson, R. J.; Weiss, E. A.; Weitz, D. A.; Whitesides, G. M. *Adv. Funct. Mater.* **2008**, *18*, 1097.

[25] Weiss, E. A.; Chiechi, R. C.; Kaufman, G. K.; Kriebel, J. K.; Li, Z.; Duati, M.; Rampi, M. A.; Whitesides G. M. *J. Am. Chem. Soc.* **2007**, *129*, 4336.

[26] Black, A. J.; Paul, K. E.; Aizenberg, J.; Whitesides, G. M. *J. Am. Chem. Soc.* **1999,** *121,* 8356.

[27] Zrnic, D.; Swatik, D. S. *J. Less-Common Met.* **1969**, *18*, 67.

[30] Venkataraman, L.; Klare, J. E.; Nuckolls, C.; Hybertsen, M. S.; Steigerwald, M. L. *Nature* **2006**, *442*, 7105.

[31] McCreery, R. L. *Chem. Mater.* **2004,** *16,* 4477.

[32] Slowinski, K.; Fong, H. K. Y.; Majda, M. *J. Am. Chem. Soc.* **1999**, *121*, 7257.

[33] Engelkes, V. B.; Beebe, J. M.; Frisbie, C. D. *J. Am. Chem. Soc.* **2004**, 126, 14287.

[34] Reus, W. F. Nijhuis, C. A.; Barber, J.; Cademartiri, L.; Mwagni, M.; Whitesides , G. M.; manuscript in preparation.

[35] Lee, S. -Y.; Tung, H. -W.; Chen, W. -C.; Fang, W. *IEEE Photon. Technol. Lett.* **2006**, *18*, 2191.

[36] Menke, Y.; Peltier-Baron, V.; Hampshire, S. *J. Non-Cryst. Solids* **2000**, *276*, 145.

[37] Yamaga, M.; Víllora, E.G.; Shimamura, K.; Ichinose, N.; Honda, M.; *Phys. Rev. B* **2003**, *68*, 155207.

[38] Lide, D. R. *Handbook of Chemistry and Physics* CRC Press, Inc.: Boca Raton, **1996**.

[39] Koster, J. N. *Cryst. Res. Technol.* **1999**, *34*, 9.

[46] Müller-Meskamp, L.; Karthäuser, S.; Zandvliet, H. J. W.; Homberger, M.; Simon, U.; Waser, R. *Small* **2009**, *5*, 496.

[47] Stadler, R.; Geskin, V.; Cornil, J. *J. Phys.: Condens. Matter.* **2008**, *20*, 374105.

[49] Creager, S. E.; Rowe, G. K. *J. Electroanal. Chem.* **1994**, *370*, 203.

---

[50] The yield of the template-stripping step was nearly 100%. We observed occasionally that the silver electrodes had defects.

Author Contributions

C.A.N. and M.D. designed and fabricated the devices. C.A.N. performed the J(V) measurements and developed the model to explain all observations. J.B. and W.F.R. repeated the fabrication, and measurements of J(V), of devices with SAMs of SC_{12} and SC_{18} and performed the AFM analysis. All authors discussed the results, commented on the manuscript, and co-wrote the paper.

Additional information

Supplementary information accompanies this paper on www.nature.com/naturematerials. Reprints and permissions information is available online at http://npg.nature.com/Reprintsandpermissions. Correspondence and requests for materials should be addressed to G.M.W.